Phonon density of states of SmS under high pressure determined by ^{149}Sm nuclear inelastic scattering

U. Ponkratz,[1,2] A. Barla,[3] J. P. Sanchez,[4] G. Lapertot,[4] R. Rüffer,[2] and G. Wortmann[1,*]
[1]*Department of Physics, University of Paderborn, D-33095 Paderborn, Germany*
[2]*European Synchrotron Radiation Facility, BP 220, F-38043 Grenoble, France*
[3]*CELLS-ALBA, E-08193 Bellaterra Barcelona, Spain*
[4]*CEA-Grenoble, INAC-SPSMS, 17 rue des Martyrs, F-38054 Grenoble, France*
(Received 18 June 2008; published 30 September 2008)

The impact of the pressure-induced valence transition on the phonon density of states (DOS) in SmS was studied by ^{149}Sm nuclear inelastic scattering of synchrotron radiation. The derived phonon DOS shows drastic differences between the divalent phase at ambient pressure and the intermediate valent phase at 1.5, 2.9, and 4.6 GPa. The phonon DOS at ambient pressure shows two peaks which can be assigned to the transverse-acoustic (TA) and longitudinal-acoustic (LA) phonon branches, while at high pressures only one broad peak is observed. The data were analyzed with a simple model for the TA and LA phonon branches, which could well describe the measured spectra. In the intermediate valent phase the pressure dependence of the cutoff energies of the TA and LA phonon branches is very different and reflects the strong modifications of the LA branches in the intermediate valent phase. This behavior is also responsible for a characteristic variation in the derived Lamb-Mössbauer factors and Debye temperatures.

DOI: 10.1103/PhysRevB.78.104120 PACS number(s): 78.70.Ck, 76.80.+y, 71.28.+d, 62.50.−p

I. INTRODUCTION

Since the discovery of its dramatic pressure-induced first-order phase transition at 0.65 GPa,[1] SmS is one of the most studied samples in the field of rare-earth (R) systems exhibiting intermediate valence (IV).[2,3] In some metallic systems and compounds of Sm, Eu, Tm, and Yb there are two possible ground states, R^{2+} and R^{3+}, and the competition between these two states can lead to an IV state showing peculiar magnetic and electronic properties connected with an unusual small bulk modulus due to the different ionic radii of the R^{2+} and R^{3+} ions and a pronounced volume change at pressure-induced valence transitions.[2,3] Sm ions can exhibit two stable configurations of the $4f$ shell, Sm^{2+} with a nonmagnetic $4f^6(^7F_0)$ ground state and Sm^{3+} with a magnetic $4f^5(^6H_{5/2})$ configuration. At ambient pressure, SmS is a nonmagnetic black semiconductor with rocksalt structure which transforms, in an isostructural first-order phase transition with a volume collapse of $\sim$15%,[1–3] to a golden metallic state with an intermediate valence of $v \approx 2.6$, increasing further up to $v \approx 3$ above 13 GPa,[4] reflecting the relative amount of the $4f^6$ and $4f^5$ configurations. Their impact on the magnetic properties has been recently investigated by some of us in a high-pressure study of SmS using nuclear forward scattering (NFS) of synchrotron radiation by the 22.494 keV resonance of ^{149}Sm.[5,6]

It was already suggested in the late 1970 that, in case of an IV state of R ions with the promotion of (part of) a $4f$ electron into the $5d$-conduction band and the concomitant change in ionic radius, the electronic configuration and binding strength should be strongly modified and reflected by corresponding modifications in the phonon-dispersion relations.[7] This has been exemplified by inelastic neutron scattering (INS) on $Sm_{0.75}Y_{0.25}S$, where an IV phase is obtained by the substitution of Sm^{2+} ions by Y^{3+} ions,[8] and in a subsequent high-pressure study of the IV phase of SmS at 0.7 GPa with a strong modification of the longitudinal-acoustic (LA) phonon branch in the [111] direction.[9] These studies triggered a description of the electron-phonon interactions by theoretical models.[10–12] The peculiar behavior of the LA [111] phonon branch was investigated recently with high accuracy by inelastic x-ray scattering (IXS) at pressures from 0.1 to 7.6 GPa.[13]

Here we studied the phonon density of states (DOS) in SmS under pressure using nuclear inelastic scattering (NIS) of synchrotron radiation by the ^{149}Sm (22.5 keV) Mössbauer resonance. The NIS method is different from the INS and IXS studies mentioned above in that it measures directly the phonon DOS without any model (e.g., Born-von Karman) and does not need single-crystalline samples.[14–16] This method was already quite often applied for the ^{57}Fe (14.4 keV) Mössbauer resonance,[16] which is most favorable for this method and also for high-pressure studies in the 100-GPa range.[17–19] NIS studies have been reported several times for other Mössbauer resonances such as ^{119}Sn and ^{151}Eu,[20–22] in part under pressure.[23,24] Due to the experimental limitations in count rate discussed below, NIS experiments with the ^{149}Sm resonance are difficult and only one study has been reported recently.[25] Here we apply the ^{149}Sm resonance to the first high-pressure NIS study of SmS, in continuation of the high-pressure ^{149}Sm-NFS studies of SmS mentioned above.[5,6]

II. EXPERIMENT

The ^{149}Sm-NIS experiments were carried out at the nuclear resonance station ID22N of the European Synchrotron Radiation Facility (ESRF) in Grenoble, France.[26] A high-resolution monochromator reduces the bandwidth of the undulator radiation down to $\Delta E = 1.0$ meV.[5] SmS powder enriched to 97% in ^{149}Sm was used in the nuclear resonant

scattering experiments. Details on the sample preparation are described in the previous ^{149}Sm-NFS studies.[5,6] All present ^{149}Sm-NIS experiments were carried out at room temperature (296 K). The resonant absorption at ambient conditions was recorded with SmS powder glued between two stripes of adhesive tape placed directly on top of an avalanche photodiode (APD) detector. High-pressure experiments were carried out using a Paderborn-type diamond-anvil cell.[17] Sample powder was loaded into a 300-μm-diameter hole of a beryllium gasket. A 4:1 methanol:ethanol mixture was used as pressure-transmitting medium. Pressures were determined using the ruby fluorescence technique.[27] Two APD detectors placed perpendicular to the beam at a distance of approximately 5 mm from the sample were used to record the resonantly scattered photons. An energy range of ± 40 meV was scanned around the ^{149}Sm resonance energy at 22.494 keV in steps of 0.25 meV. Due to the unfavorable nuclear parameters of the ^{149}Sm resonance, here with a short lifetime (τ=10.3 ns), which uses less than 10% of the bunch separation time of 176 ns at the ESRF,[26] and a high internal-conversion coefficient (α=50) together with the low energy of the successive *L*-x rays, which are strongly absorbed within the SmS sample, the inelastic count rates are rather low, e.g., 20 Hz in the wings of the NIS spectra around 10 meV at ambient pressure and reduced to about 1 Hz in the high-pressure experiments. At high pressure, typically about 40 spectra, each collected in about 30 min, were measured and summed up afterward.

III. RESULTS AND DISCUSSION

The ^{149}Sm-NIS spectra of SmS at ambient conditions and at 1.5, 2.9, and 4.6 GPa are shown in Fig. 1. After background subtraction, the spectra were normalized so that the first moment of each spectrum equals the recoil energy of a free ^{149}Sm nucleus E_R=1.832 meV.[28] For SmS at ambient pressure the NIS spectrum shows two well separated peaks at ± 10 and ± 13 meV. According to the phonon-dispersion relations determined by inelastic neutron scattering[3,7] we can assign these peaks to the cutoff frequencies of the transverse-acoustic and longitudinal-acoustic branches, respectively. The optical phonons branches[3,7] reported in the neutron study at energies between 22 and 26 meV (transverse-optical mode) and around 30 meV (longitudinal-optical mode) are not observed in the present study. NIS is an isotope-selective method and therefore only sensitive to vibrations of the Sm atoms. Due to the large mass ratio of Sm to S, the displacements of the Sm atoms due to optical phonons are much smaller than due to acoustic phonons, thus making optical phonons difficult to detect by ^{149}Sm NIS.

As demonstrated in the upper part of Fig. 1, the NIS spectrum of SmS in the IV phase at 1.5 GPa is strongly different from the spectrum at ambient pressure. In particular, the resolved double-peak structure changed to a rather broad peak around 12 meV. The NIS spectra of SmS at 2.9 and 4.6 GPa are similar to the spectrum at 1.5 GPa, but the statistical accuracy is limited due to the low count rate. However, a shift of the high-energy flank to larger energy values with pressure is clearly observable.

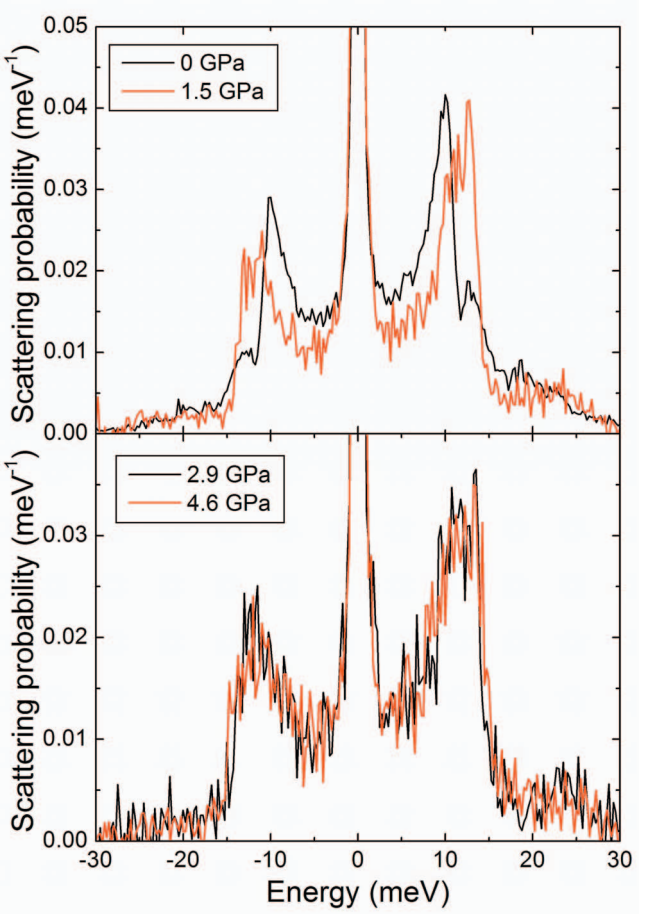

FIG. 1. (Color) The measured ^{149}Sm-NIS spectra of SmS at four different pressure values.

In order to extract the Sm phonon DOS we used a software code based on the theory described in Ref. 29. The extraction of the Sm partial phonon DOS worked very well for the data taken at ambient conditions and at 1.5 GPa. The derived phonon DOS represents very well the spectral features displayed in Fig. 1. The data taken on SmS at 2.9 and 4.6 GPa were more difficult to analyze due to the low statistical accuracy. The derived phonon DOS at 2.9 and 4.6 GPa is similar to the one at 1.5 GPa but broadened and shifted to higher energies.

From the phonon DOS of SmS shown in Fig. 2 we calculated some of the elastic and thermodynamic parameters of the Sm sublattice as described in detail in Refs. 29 and 30. The so-called high-temperature Debye temperature $\Theta_{\text{D-HT}}$ is proportional to the first moment of the phonon DOS given by

$$\Theta_{\text{D-HT}} = \frac{4}{3}\frac{1}{k_B}\int_0^\infty g(E)E dE. \quad (1)$$

Here, k_B is Boltzmann constant. The mean force constant D can be calculated from the second momentum of the phonon DOS with $M=2.474\times10^{-25}$ kg being the mass of the ^{149}Sm nucleus;

$$D = \frac{M}{\hbar^2}\int_0^\infty g(E)E^2 dE. \quad (2)$$

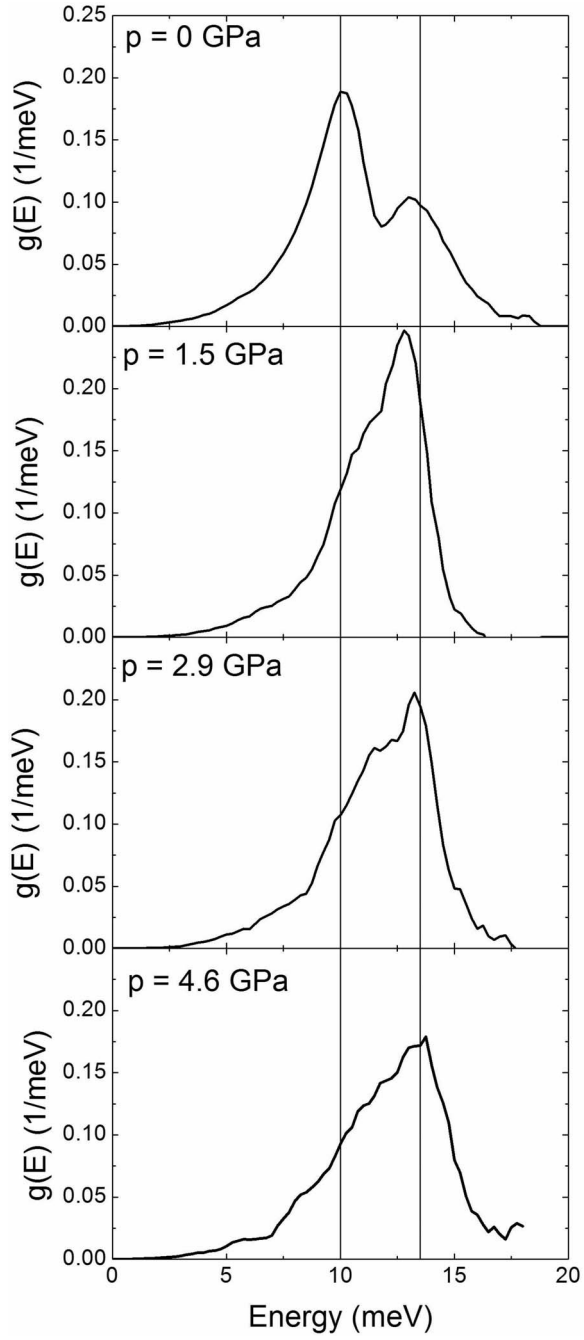

FIG. 2. The Sm phonon DOS of SmS at four different pressures as obtained from the measured NIS spectra. The data were smoothed by averaging five adjacent points.

A very useful elastic parameter is the Lamb-Mössbauer factor f_{LM}, which describes the fraction of recoilless absorbed photons in nuclear resonant absorption processes observed by traditional Mössbauer spectroscopy in the temperature dependence of the absorption area of the resonance spectra. In the present case, the Lamb-Mössbauer factor f_{LM} at the experimental temperature (here $T=296$ K) can be calculated from the phonon DOS by

$$f_{\mathrm{LM}} = \exp\left(-E_R \int_0^\infty \frac{g(E)}{E} \frac{1+e^{-\beta E}}{1-e^{-\beta E}} dE\right). \tag{3}$$

TABLE I. Thermodynamic and elastic parameters of the Sm sublattice in SmS calculated from the derived Sm phonon DOS measured at 296 K. Here $\Theta_{\mathrm{D\text{-}HT}}$ is the high-temperature Debye temperature, D the mean force constant, f_{LM} the Lamb-Mössbauer factor, and $\langle x^2\rangle$ the mean-square displacement for the Sm sublattice.

	0 GPa	1.5 GPa	2.9 GPa	4.6 GPa
$\Theta_{\mathrm{D\text{-}HT}}$ (K)	166(3)	175(5)	180(7)	190(7)
D (N/m)	71(6)	75(8)	78(10)	78(10)
f_{LM}	0.29(1)	0.38(1)	0.39(2)	0.40(2)
$\langle x^2\rangle(10^{-24}$ m$^2)$	95(3)	75(3)	73(5)	71(5)

Here, $E_R=1.823$ meV is the recoil energy of a free ^{149}Sm nucleus and $\beta=1/(k_BT)$. The mean-square displacement of the Mössbauer atom $\langle x^2\rangle$ can be calculated from the Lamb-Mössbauer factor using the following relation with $k=1.140\times10^{11}$ m^{-1} for the wave vector of the gamma radiation:

$$\langle x^2\rangle = \frac{-\ln(f_{\mathrm{LM}})}{k^2}. \tag{4}$$

The derived parameters from Eqs. (1)–(4) are given in Table I. In the following we discuss the behavior of these parameters of SmS at the valence transition from the data obtained at 0 and 1.5 GPa. The Debye temperature $\Theta_{\mathrm{D\text{-}HT}}$, derived from the first moment of the whole phonon DOS, increases from 166 to 175 K by only 5.4%. This change is small compared to the large volume change of $\Delta V/V$ by 16% between 0 and 1.5 GPa. This behavior reflects, similar to that of the mean force constant D with larger error bars, the unusual elastic properties of the IV phase, in particular of the LA branches on the high-energy side of the phonon DOS, to be discussed later. On the other hand, the increase in the Lamb-Mössbauer factor f_{LM} from 0.29 to 0.38 between 0 and 1.5 GPa is the magnitude to be expected from the behavior of the low-energy part of the phonon DOS in Fig. 2 dominated by the contributions of the TA phonon branches. The mean-square displacement of the Sm atoms $\langle x^2\rangle$ shows a corresponding decrease from $95(3)\times10^{-24}$ to $75(3)\times10^{-24}$ m^2 at the valence transition. It should be mentioned that the value of $\langle x^2\rangle$ at ambient pressure agrees very well with $100(9)\times10^{-24}$ m^2 derived for the Sm atoms in SmS at 300 K in a single-crystal x-ray diffraction study,[31] demonstrating the reliability of present NIS results. A value of $\langle x^2\rangle$ given in this study[31] for $Sm_{0.7}Y_{0.3}S$ in the IV state at 300 K cannot be compared directly with our value because the structural disorder induced by the Y^{3+} ions contributes considerably to $\langle x^2\rangle$. A theoretical value of 85×10^{-24} m^2 derived without structural disorder[31] compares favorably with the above value at 1.5 GPa when the difference in the lattice parameters is taken into account. One should emphasize that the "pure" pressure-induced IV phase of SmS is different in the elastic and electronic properties from the IV phases of $Sm_{1-x}Y_xS$ systems, as pointed out in the above-mentioned studies[3,9] as well as in the pioneering ^{149}Sm-Mössbauer study of the pressure-induced valence transition in SmS and comparison with $Sm_{1-x}Y_xS$.[32] Finally we want to mention

that the Sm phonon DOS in Fig. 2 and the derived parameters given in Table I, to be discussed later in Fig. 5, represent integral properties and were derived without using any phonon-dispersion models.

In the following we show a different way to analyze the NIS data in order to obtain information on the behavior of the longitudinal and transverse phonon branches under pressure. Usually one extracts the phonon DOS from the measured NIS spectra using a mathematical algorithm.[29] One can also do it "vice versa," i.e., starting from a theoretical model for the phonon DOS describing the longitudinal and transverse phonon branches by simple assumptions. With such a model and calculating the multiphonon contributions and taking into account the detailed balance of temperature and the energy dependence of phonon excitations and deexcitations, one can reconstruct the measured NIS spectra. Treating the model parameters as fitting variables one can compare the calculated and measured NIS data. Before introducing the model we want to emphasize that a simple phonon DOS according to the Debye model with an E^2 dependence over the whole energy range up to the cutoff energy E_D, which split into two contributions from transverse and longitudinal branches with cutoff energies $E_{D,T}$ and $E_{D,L}$, cannot describe the actual phonon DOS of a real solid.

In the Appendix we introduce a simple model for the phonon DOS according to a three-dimensional harmonic chain model. The derived phonon DOS is given by

$$g(E) = \frac{2}{3} g_{TA}(E, E_{max,TA}) + \frac{1}{3} g_{LA}(E, E_{max,LA}). \quad (5)$$

The contribution of TA and LA phonons to the total phonon DOS are represented by the terms $g_{TA}(E, E_{max,TA})$ and $g_{LA}(E, E_{max,LA})$, respectively. $E_{max,TA}$ and $E_{max,LA}$ are the maximum energies of both TA and LA phonon branches. The function $g(E, E_{max})$ is defined as (see the Appendix)

$$g(E, E_{max}) = \frac{24}{\pi^3} \frac{1}{E_{max}} \frac{\arcsin^2(E/E_{max})}{\sqrt{1-(E/E_{max})^2}}. \quad (6)$$

In the following we will explain the different steps in calculating the NIS spectrum starting from this phonon DOS model for the TA and LA branches [see Fig. 3(a)]. The two van Hove singularities correspond to the cutoff energies $E_{max,TA}$ and $E_{max,LA}$ of the TA and the LA branches, respectively. Starting from this model, the one-phonon $S_1(E)$ and multiphonon $S_n(E)$ contributions to the NIS spectrum can be calculated. $S_1(E)$ is given by $S_1(E) = E_R g(|E|)/E(1-e^{-\beta E})$ (Ref. 28) where β is defined as in Eq. (3). The calculation of two-phonon $S_2(E)$ and higher terms $S_n(E)$ is more complicated since it requires the computation of convolution integrals. A more detailed description can be found in the literature.[28] In Fig. 3(b) we show the calculated one- and two-phonon terms of inelastic scattering at 300 K. The total scattering is given by the sum of all multiphonon terms [Fig. 3(c)]. In the present case, with a Lamb-Mössbauer factor of about 0.3, it is sufficient to take into account multiphonon terms only up to three-phonon interactions; higher terms are negligible. Finally, the calculated NIS spectrum is convoluted with the experimental resolution function [Fig. 3(d)].

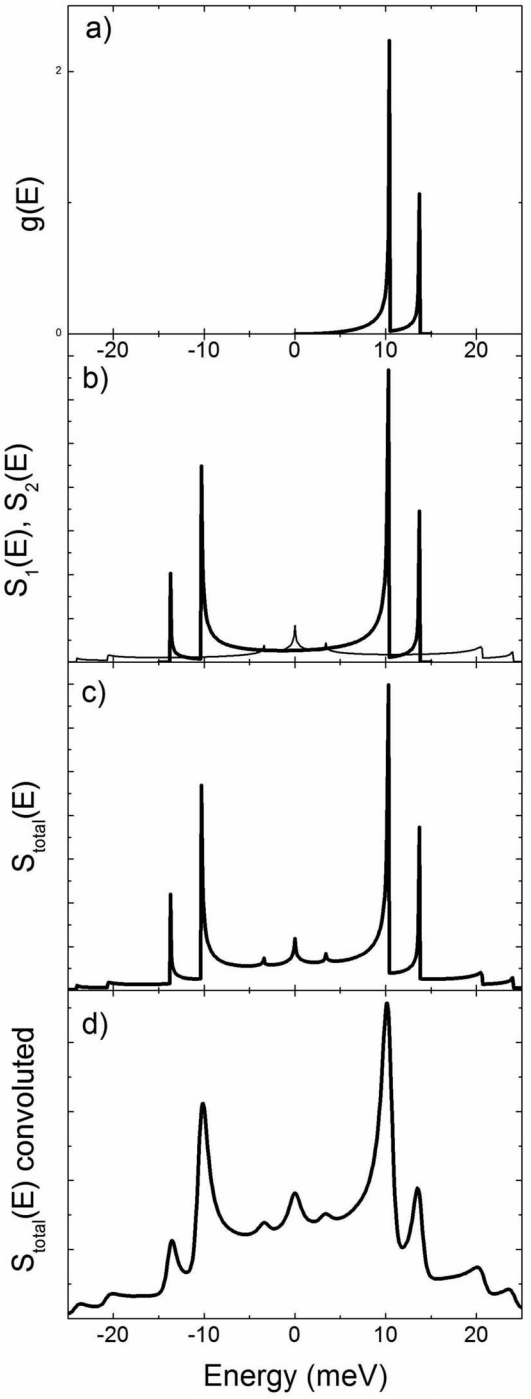

FIG. 3. The phonon DOS according to the three-dimensional linear-chain model is shown in (a). The calculated one-phonon $S_1(E)$ (thick line) and two-phonon (thin line) contributions $S_2(E)$ are shown in (b). In (c), the calculated NIS spectrum including up to three phonons is shown. Finally, (d) shows the theoretical NIS spectrum convoluted with the experimental resolution function with the full width at half maximum of 1 meV.

The function shown in Fig. 3(d) already represents the basic features of the measured NIS spectrum at ambient pressure [Fig. 1(a)]. A good agreement with the NIS spectrum at ambient pressure is then obtained by a convolution of the model function with an additional Gaussian function with a width

of 1 meV. This additional convolution takes into account the elastic anisotropy of a real three-dimensional solid, e.g., the different crystallographic directions shown and discussed in experimental and theoretical works.[7–12]

The final results of the fit to the NIS spectra are shown in Fig. 4. The data at ambient pressure are well matched with this model, in particular the clear separation between the TA and LA branches with fitted cutoff energies of 10.3(1) and 13.7(1) meV. Comparison with inelastic neutron-scattering data shows that the derived energies match well the average of the maximum frequencies of the TA and LA branches.[3,7]

The NIS spectrum of IV SmS at 1.5 GPa, drastically different from the one at ambient pressure, is also well described with this model. For the TA branch, the cutoff energy *increases* from 10.3 to 12.1(2) meV, while the cutoff energy of the LA branch *decreases* slightly from 13.7 to 13.4(1) meV. The unusual behavior of the LA branch at the transition to the IV state in agreement with the results of inelastic neutron scattering and especially with recent detailed IXS data.[13] The latter found a decrease in the phonon cutoff frequency of the LA [111] branch from 15.7 to 14.3 meV above the phase transition at 0.9 GPa. Since our analysis represents an average of all crystallographic directions, this unusual decrease in energy of the LA branch is less pronounced but still observable.

Since the present model describes well the IV state of SmS at 1.5 GPa, we used the same approach to analyze the NIS spectra measured with lower statistical accuracy at 2.9 and 4.6 GPa. The cutoff energy of the LA branch increases now strongly from 13.9(2) meV (2.9 GPa) to 14.7(2) meV (4.6 GPa), while the cutoff energy of the LA branch increases less pronounced from 12.3(2) meV (2.9 GPa) to 12.5(2) meV (4.6 GPa). The derived data of E_{max} for the TA and LA branches are shown in Fig. 5 and can be used to calculate the mode-Grüneisen parameters $\gamma = -\partial \ln E_{max} / \partial \ln V$ in the IV phase. The Grüneisen parameters were obtained by a linear interpolation of the E_{max} values in the IV phase and from the lattice parameters of SmS under pressure.[33] For the volume change of 4.1% between 1.5 and 4.6 GPa we observe quite different shifts of E_{max}, which result in values of $\gamma_{LA}=2.2(4)$ for the LA branch and $\gamma_{TA}=0.9(6)$ for the TA branch. This rather high value for γ_{LA} reflects the large values of $\gamma_{LA\ [111]}$ observed for the LA [111] mode in the IV phase between 0.9 and 7.6 GPa in the above-mentioned IXS study.[13] On the other hand, the value of γ_{TA} shows normal behavior such as the variation in $E_{max,TA}$ at the valence transition. This drastically different behavior of both the E_{max} and γ values between the LA and TA branches reflects the sensitivity of the LA modes to the changes connected with the Sm ionic radii and valence-band structure in the IV phase discussed in previous studies.[8–13,33] In a similar way, a Grüneisen parameter can be calculated for the Debye temperature $\Theta_{D\text{-}HT}$ in the IV phase using the relation $\gamma_{\Theta\text{-}HT} = -\partial \ln \Theta_{D\text{-}HT} / \partial \ln V$. In this case the result is $\gamma_{\Theta\text{-}HT}=1.9(5)$ (see Fig. 5). Since $\Theta_{D\text{-}HT}$ is calculated from the first energy moment of the phonon DOS, the contribution of the LA branch is more pronounced and the value of $\gamma_{\Theta\text{-}HT}$ is close to the value of γ_{LA}. On the other hand, the Lamb-Mössbauer factor, determined mainly from the TA branches as mentioned above, exhibits a linear variation over the whole pressure range comparable with the energy variation in the TA branch (see Fig. 5).

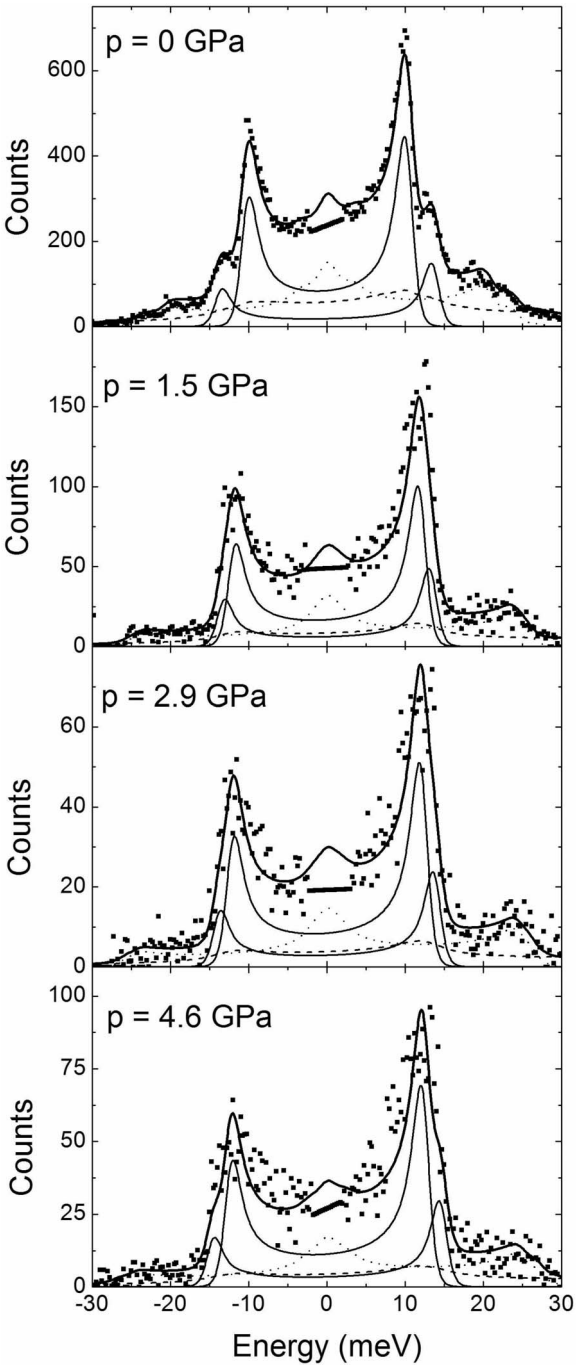

FIG. 4. NIS spectra of SmS at different pressures. The lines are fits to the data using the three-dimensional linear-chain model as described in the text. The solid lines correspond to single-phonon excitations due to TA and LA phonons. The dotted line and the dashed line correspond to the two- and three-phonon contributions, respectively. The thick solid line represents the sum over all contributions.

IV. SUMMARY

We have applied the method of ^{149}Sm NIS for studying the local phonon DOS in SmS at the pressure-induced va-

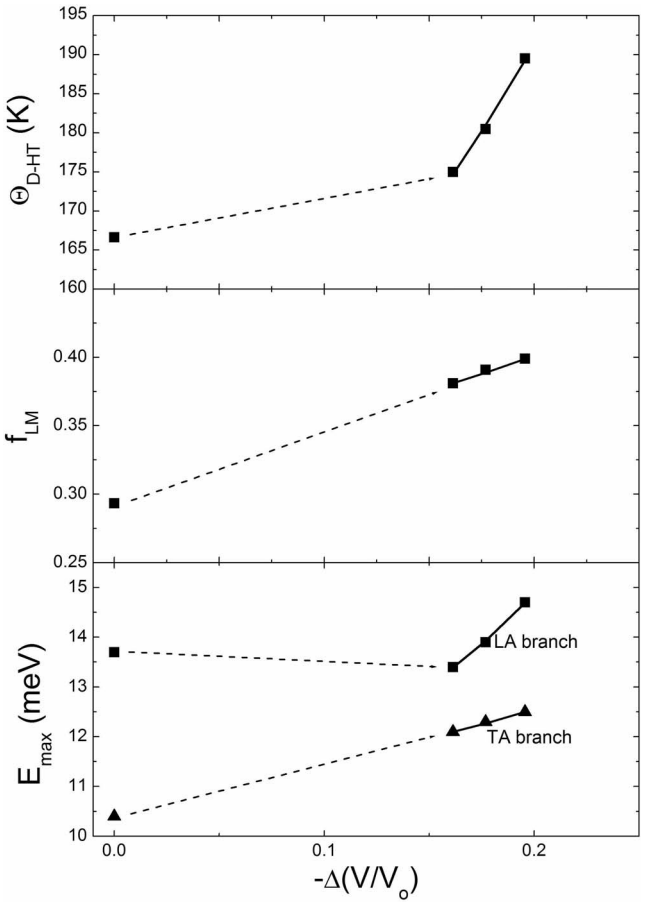

FIG. 5. Volume dependence of (above) the high-temperature Debye temperature $\Theta_{\text{D-HT}}$ and (middle) the Lamb-Mössbauer factor f_{LM}, both derived from the phonon DOS, as well as (below) the cutoff energies $E_{\max}$ of the TA branch and LA branch derived from the analysis of the NIS spectra as described in the text. The error bars of the data are given in Table I and for $E_{\max}$ in the text.

lence transition. The derived Sm phonon DOS shows drastic changes between the ambient pressure phase and the high-pressure IV phase. From the phonon DOS we derived elastic and thermodynamic parameters such as the Lamb-Mössbauer factor and the Debye temperature of the Sm sublattice. Both parameters show characteristic changes at the valence transition and in the IV phase reflecting the impact of the TA phonon and LA phonon branches, respectively. In order to extract detailed information on the TA and LA branches from the measured NIS spectra we introduced a simple model based on a harmonic linear-chain model expanded to three dimensions. It allows us to follow the cutoff energies of both TA and LA phonon branches in the divalent and the IV phase of SmS. With this simple model we derived cutoff energies $E_{\max,\text{TA}}$ and $E_{\max,\text{LA}}$ which represent average values for the TA and LA branches in different crystallographic directions. The general behavior of $E_{\max,\text{TA}}$ and $E_{\max,\text{LA}}$ derived in the present approach is in good agreement with the results of previous inelastic neutron and IXS studies investigating only selected phonon branches. In particular, the unusual behavior of the LA [111] branch is also reflected by a decrease in $E_{\max,\text{LA}}$ at the valence transition followed by a strong increase with pressure in the IV phase. The different variations in the TA and LA phonon branches through the valence transition and within the IV phase, documented by different Grüneisen parameters, is also reflected by the variations in the Lamb-Mössbauer factor and in the Debye temperature, respectively, derived directly from the phonon DOS.

ACKNOWLEDGMENTS

Two of us (U.P. and G.W.) gratefully acknowledge financial support from the German BMBF (Grant No. 05KS4PPB/4). We would like to thank Svetoslav Stankov, Cornelius Strohm, and Ilya Sergueev for their help in setting up the beamline for the ^{149}Sm resonance.

APPENDIX

We introduce here a simple model to describe the overall spectral shape of nuclear resonant scattering at the acoustic branches in an isotropic three-dimensional system.

We start with the one-dimensional linear-chain model, where the vibration energy as a function of the momentum k is given by[34]

$$E(k) = \frac{2\hbar}{\pi} v \sin\left(\frac{\pi}{2}\frac{k}{k_{\max}}\right) k_{\max}. \tag{A1}$$

The maximum momentum $k_{\max}$ corresponds to the zone boundary in the reciprocal space and v is the sound velocity in the long-wavelength limit. This relation can be applied for the one-atomic chain and for the acoustic branches, and also for a two-atomic chain. The sound velocity v is related to the effective mass M and the force constant D by

$$v = \frac{\pi}{k_{\max}}\sqrt{\frac{D}{M}}. \tag{A2}$$

The phonon dispersion is proportional to a sine function with a maximum energy of

$$E_{\max} = \frac{2\hbar}{\pi} v k_{\max}. \tag{A3}$$

For the following it is more useful to work with the relation $k(E)$ for the phonon dispersion, which is obtained by inverting Eq. (A1):

$$k(E) = \frac{E_{\max}}{\hbar v}\arcsin(E/E_{\max}). \tag{A4}$$

The next step is to expand this one-dimensional model to three dimensions. Although it was proven that SmS is elastically anisotropic with an anisotropy ratio of $A = C_{44}/C' = 0.47$,[35] we will treat, in first approximation, SmS as an elastically isotropic solid. In this case, in three dimensional reciprocal space the number of states N having a momentum k is assumed to be proportional to a sphere with radius k;

$$dN(k) \propto 4\pi k^2 dk. \tag{A5}$$

Using formula (A5) and calculating the differential dk/dE from (A4), one finds

$$dN \propto \frac{E_{\max}^2}{\hbar^3 v^3} \frac{\arcsin^2(E/E_{\max})}{\sqrt{1-(E/E_{\max})^2}} dE. \quad \text{(A6)}$$

The phonon density of states $g(E)$ is proportional to dN/dE. The correct prefactor can be found by taking into account the usual normalization

$$\int_0^{E_{\max}} g(E)dE = 1. \quad \text{(A7)}$$

Finally, the normalized phonon DOS is given by

$$g(E,E_{\max}) = \frac{24}{\pi^3} \frac{1}{E_{\max}} \frac{\arcsin^2(E/E_{\max})}{\sqrt{1-(E/E_{\max})^2}}. \quad \text{(A8)}$$

Up to now it was assumed that there is only one-phonon branch. In a real solid there are two TA and one LA phonon branches. This is taken account by using two-phonon DOS with two maximum energies $E_{\max,\mathrm{TA}}$ and $E_{\max,\mathrm{LA}}$. The normalization is respected by weighting the two sub-DOS by using the appropriate prefactors of 2/3 and 1/3, respectively,

$$g(E) = \frac{2}{3} g_{\mathrm{TA}}(E,E_{\max,\mathrm{TA}}) + \frac{1}{3} g_{\mathrm{LA}}(E,E_{\max,\mathrm{LA}}). \quad \text{(A9)}$$

We want to mention that the present simple model with only one TA and one LA branch, averaged over all crystallographic directions, is only applicable to describe the phonon DOS in a simple (cubic) crystal structure with a (pseudo) one-atomic base, as in the present case of SmS. The elastic anisotropy of a real three-dimensional crystal will be considered later by an appropriate broadening of the spectral features (see text).

*Corresponding author; wortmann@physik.upb.de

[1] A. Jayaraman, V. Narayanamurti, E. Bucher, and R. G. Maines, Phys. Rev. Lett. **25**, 1430 (1970).

[2] *Valence Instabilities and Related Narrow Band Phenomena*, edited by R. D. Parks (Plenum, New York, 1997).

[3] P. Wachter, in *Handbook on the Physics and Chemistry of Rare Earths*, edited by K. A. Gschneidner, Jr., L. Eyring, G. H. Lander, and G. R. Choppin (Elsevier, Amsterdam, 1994), Vol. 19, p. 177.

[4] E. Annese, A. Barla, C. Dallera, G. Lapertot, J. P. Sanchez, and G. Vanko, Phys. Rev. B **73**, 140409(R) (2006).

[5] A. Barla, J. P. Sanchez, Y. Haga, G. Lapertot, B. P. Doyle, O. Leupold, R. Rüffer, M. M. Abd-Elmeguid, R. Lengsdorf, and J. Flouquet, Phys. Rev. Lett. **92**, 066401 (2004).

[6] A. Barla, J. P. Sanchez, J. Derr, B. Salce, G. Lapertot, J. Flouquet, B. P. Doyle, O. Leupold, R. Rüffer, M. M. Abd-Elmeguid, and R. Lengsdorf, J. Phys.: Condens. Matter **17**, S837 (2005).

[7] R. J. Birgenau and S. M. Shapiro, in Ref. 2, p. 49.

[8] H. A. Mook, R. M. Nicklow, T. Penney, F. Holtzberg, and M. W. Shafer, Phys. Rev. B **18**, 2925 (1978); H. A. Mook and R. M. Nicklow, *ibid.* **20**, 1656 (1979).

[9] H. A. Mook, D. B. McWhan, and F. Holtzberg, Phys. Rev. B **25**, 4321 (1982).

[10] H. Bilz, G. Güntherodt, W. Kleppmann, and W. Kress, Phys. Rev. Lett. **43**, 1998 (1979).

[11] P. Entel, N. Grewe, M. Sietz, and K. Kowalski, Phys. Rev. Lett. **43**, 2002 (1979).

[12] T. Matsuura, R. Kittler, and K. H. Bennemann, Phys. Rev. B **21**, 3467 (1980).

[13] S. Raymond, J. P. Rueff, M. D'Astuto, D. Braithwaite, M. Krisch, and J. Flouquet, Phys. Rev. B **66**, 220301(R) (2002).

[14] M. Seto, Y. Yoda, S. Kikuta, X. W. Zhang, and M. Ando, Phys. Rev. Lett. **74**, 3828 (1995).

[15] W. Sturhahn, T. S. Toellner, E. E. Alp, X. Zhang, M. Ando, Y. Yoda, S. Kikuta, M. Seto, C. W. Kimball, and B. Dabrowski, Phys. Rev. Lett. **74**, 3832 (1995).

[16] A. I. Chumakov and W. Sturhahn, Hyperfine Interact. **123/124**, 781 (1999).

[17] R. Lübbers, H. F. Grünsteudel, A. I. Chumakov, and G. Wortmann, Science **287**, 1250 (2000).

[18] H. K. Mao, J. Xu, V. V. Struzhkin, J. Shu, R. J. Hemley, W. Sturhahn, M. Y. Hu, E. E. Alp, L. Vocadlo, D. Alfé, G. D. Price, M. J. Gillan, M. Schwoerer-Böhning, D. Häusermann, P. Eng, G. Shen, H. Giefers, R. Lübbers, and G. Wortmann, Science **292**, 914 (2001).

[19] H. Giefers, R. Lübbers, K. Rupprecht, G. Wortmann, D. Alfè, and A. I. Chumakov, High Press. Res. **22**, 501 (2002); H. Giefers, G. Wortmann, A. I. Chumakov, and D. Alfè, in *ESRF Highlights 2004*, edited by G. Admans (ESRF, Grenoble, 2005), p. 18.

[20] A. Barla, R. Rüffer, A. I. Chumakov, J. Metge, J. Plessel, and M. M. Abd-Elmeguid, Phys. Rev. B **61**, R14881 (2000).

[21] G. J. Long, R. P. Hermann, F. Grandjean, E. E. Alp, W. Sturhahn, Ch. E. Johnson, D. E. Brown, O. Leupold, and R. Rüffer, Phys. Rev. B **71**, 140302(R) (2005).

[22] R. P. Hermann, W. Schweika, O. Leupold, R. Rüffer, G. S. Nolas, F. Grandjean, and G. J. Long, Phys. Rev. B **72**, 174301 (2005).

[23] H. Giefers, S. Koval, G. Wortmann, W. Sturhahn, E. E. Alp, and M. Y. Hu, Phys. Rev. B **74**, 094303 (2006).

[24] H. Giefers, E. A. Tanis, S. P. Rudin, C. Greeff, X. Ke, C. Chen, M. F. Nicol, M. Pravica, W. Pravica, J. Zhao, A. Alatas, M. Lercher, W. Sturhahn, and E. Alp, Phys. Rev. Lett. **98**, 245502 (2007).

[25] S. Tsutsui, J. Umemura, H. Kobayashi, Y. Yoda, H. Onodera, H. Sugawara, D. Kikuchi, H. Sato, C. Sekine, and I. Shirotani, Physica B (Amsterdam) **383**, 142 (2006).

[26] R. Rüffer and A. I. Chumakov, Hyperfine Interact. **97/98**, 589 (1996).

[27] H. K. Mao, P. M. Bell, J. W. Shaner, and D. J. Steinberg, J. Appl. Phys. **49**, 3276 (1978).

[28] A. I. Chumakov, R. Rüffer, A. Q. R. Baron, H. Grünsteudel, and H. F. Grünsteudel, Phys. Rev. B **54**, R9596 (1996).

[29] V. G. Kohn and A. I. Chumakov, Hyperfine Interact. **125**, 205 (2000).

[30] R. Rüffer and A. I. Chumakov, Hyperfine Interact. **128**, 255 (2000).

[31] P. D. Dernier, W. Weber, and L. D. Longinotti, Phys. Rev. B **14**, 3635 (1976).
[32] J. M. D. Coey, S. K. Ghatak, M. Avignon, and F. Holtzberg, Phys. Rev. B **14**, 3744 (1976).
[33] R. Keller, G. Güntherodt, W. B. Holzapfel, M. Dietrich, and F. Holtzberg, Solid State Commun. **29**, 753 (1979).
[34] N. W. Ashcroft and N. D. Mermin, *Solid State Physics* (Saunders, Fort Worth, 1976).
[35] Tu Hailing, G. A. Saunders, and H. Bach, Phys. Rev. B **29**, 1848 (1984).